

1 Capabilities of the Lamont-Doherty Earth Observatory *in situ*  $^{14}\text{C}$  extraction  
2 laboratory updated

3

4 Brent M Goehring<sup>1,\*</sup>, Irene Schimmelpfennig<sup>1</sup>, Joerg M Schaefer<sup>1</sup>

5 <sup>1</sup>Lamont-Doherty Earth Observatory of Columbia University, Palisades, NY 10964

6 \* Now at Dept. of Earth, Atmospheric, and Planetary Sciences, Purdue University, West  
7 Lafayette, IN 47907

8

9 Abstract

10 We report on the status and capabilities of the Lamont-Doherty Earth Observatory  
11 *in situ*  $^{14}\text{C}$  extraction laboratory. In late 2006 we began, in collaboration with the AMS  
12 group at the University of Arizona, construction of a new laboratory to extract *in situ*  
13 cosmogenic  $^{14}\text{C}$  from terrestrial silicates. Long-term measurements of the process blank  
14 over the last two years give an arithmetic mean and standard deviation of  $125 \pm 43 \times 10^3$   
15 atoms  $^{14}\text{C}$  ( $n=9$ ) and show significant improvement in the number of atoms, as well as  
16 stability compared to initial measurements of the process blank. We report long-term  
17 measurements of the intercomparison material CRONUS-A, which has been developed  
18 as part of the CRONUS-Earth effort to characterize inter- and intra-laboratory variability.  
19 We interpret the standard deviation (5%) of six replicate measurements of CRONUS-A  
20 as the reproducibility of *in situ*  $^{14}\text{C}$  extractions in our laboratory.

21 Introduction

22 Like the other commonly measured cosmogenic nuclides,  $^{14}\text{C}$  is produced *in situ* in  
23 earth surface materials by secondary cosmic rays. *In situ*  $^{14}\text{C}$  has a number of advantages  
24 over the other commonly measured cosmogenic nuclides: It has the shortest half-life  
25 (5730 yrs), making it uniquely suited to address a number of questions either on its own  
26 or in concert with a longer-lived nuclide (e.g., paired  $^{10}\text{Be}$ - $^{14}\text{C}$  measurements).  
27 Production of *in situ*  $^{14}\text{C}$  in quartz is at a rate approximately three times that of  $^{10}\text{Be}$

28 (Dugan et al., 2008; Lifton et al., 2001; Miller et al., 2006; Schimmelpfennig et al., 2012).  
29 The measurement sensitivity of  $^{14}\text{C}$  is currently greater than all of the other cosmogenic  
30 nuclides, except for  $^3\text{He}$ , and the abundance of accelerator mass spectrometry (AMS)  
31 facilities with  $^{14}\text{C}$  measurement capability is far greater than for the other nuclides. The  
32 above factors make *in situ*  $^{14}\text{C}$  a potentially powerful tool in the study of earth surface  
33 processes.

34 The most promising application of *in situ*  $^{14}\text{C}$  is when it is paired with one or  
35 more longer-lived cosmogenic nuclides to investigate complex exposure histories during  
36 the past ca. 30 ka. To date only a few studies using *in situ*  $^{14}\text{C}$  have been published, all  
37 but one in the field of glacial geology (Anderson et al., 2008; Goehring et al., 2011;  
38 Miller et al., 2006; White et al., 2011), the other used *in situ*  $^{14}\text{C}$  to assess inherited  $^{10}\text{Be}$   
39 (Matmon et al., 2005). Further potential applications of this paired nuclide approach are  
40 broad and include studies of soil column overturning rates/depths (Fülöp et al., 2009;  
41 Hippe et al., 2012; Lal et al., 1996), and paleoseismology (Handwerger et al., 1999). The  
42 refinement of models of nucleon scaling is another promising field for *in situ*  $^{14}\text{C}$  due to  
43 its relatively rapid achievement of secular equilibrium (Brook et al., 1995; Lifton et al.,  
44 2008). Determinations of the  $^{14}\text{C}$  production rates in quartz are also scarce (Dugan et al.,  
45 2008; Lifton et al., 2001; Miller et al., 2006; Schimmelpfennig et al., 2012). The paucity  
46 of studies employing *in situ*  $^{14}\text{C}$  reflects both the limited number of laboratories with *in*  
47 *situ*  $^{14}\text{C}$  extraction capabilities and the challenge of low-background extraction (Fülöp et  
48 al., 2010; Goehring et al., 2008; Hippe et al., 2009; Lifton et al., 2001; Pigati et al., 2010).

49 In 2006 we began construction of a new *in situ*  $^{14}\text{C}$  laboratory at Lamont-Doherty  
50 Earth Observatory of Columbia University (LDEO). Development of the laboratory

51 facilities is complete and in a stable operating mode since 2010. Here we report on  
52 progress made in the laboratory, including blank levels, improvements in precision, and  
53 measurements of a recently developed intercomparison material.

#### 54 Lab Design and Extraction Procedures

55 All extraction, purification, and graphitization lines are based on the designs of  
56 Lifton et al. (2001) and Pigati et al. (2010). The laboratory is comprised of three main  
57 systems, a flow-through extraction line (Pigati et al., 2010), a purification line (Lifton,  
58 2001), and dedicated *in situ*  $^{14}\text{C}$  graphitization line (Slota et al., 1987).

59 Extraction of *in situ*  $^{14}\text{C}$  from quartz and preparation for AMS analysis is a three-  
60 day process and follows the procedure outlined in Pigati et al. (2010). Day one consists of  
61 a 1 hour  $1200^{\circ}\text{C}$  combustion of the lithium meta-borate ( $\text{LiBO}_2$ ) flux and alumina  
62 combustion boat to remove any surface contaminants and initially degass the  $\text{LiBO}_2$ . The  
63  $\text{LiBO}_2$  is used to reduce the quartz fusion temperature during the subsequent sample  
64 combustion (Lifton et al., 2001). Day one  $\text{LiBO}_2$  combustion is done at  $1200^{\circ}\text{C}$  to ensure  
65 release of all potential contaminants; however, combustion at  $1100^{\circ}\text{C}$ , which is the  
66 sample combustion temperature should be equally effective. All evolved carbon species  
67 are converted to  $\text{CO}_2$  under a 5 sccm flow of ultra-high-purity  $\text{O}_2$  held at 50 torr ( $\sim 6.7$   
68 kPa) via interaction with 2-mm quartz beads within a u-tube furnace held at  $1000^{\circ}\text{C}$ . This  
69 removes surface and atmospheric carbon contaminates from the flux as well as the  
70 combustion boat and quartz sleeve, which protects the mullite furnace tube from the  
71 volatile  $\text{LiBO}_2$ . On day two,  $\sim 5$  g of quartz is added to the combustion boat and the  
72 sample and flux are heated at  $500^{\circ}\text{C}$  for 1 hour to remove atmospheric carbon  
73 contaminates, again in the presence of a 5 sccm flow of  $\text{O}_2$ . The sample is then heated at

74 1100°C for two hours in the presence of 50 torr (~6.7 kPa; static) of O<sub>2</sub>, this melts the  
75 LiBO<sub>2</sub> and dissolves the quartz, releasing carbon. Following the initial two hour  
76 combustion, the sample is held at 1100°C for another hour in the presence of a 5 sccm  
77 flow of O<sub>2</sub>, while a 50 torr (~6.7 kPa) tube pressure is maintained. All evolved CO<sub>2</sub> is  
78 collected in a liquid nitrogen-cooled coil trap and transferred to a flame-cleaned breakseal  
79 for subsequent gas purification. Day three involves the purification of the CO<sub>2</sub> by  
80 cryogenic removal of contaminant species (e.g. H<sub>2</sub>O, NO<sub>x</sub>, SO<sub>2</sub>, SO<sub>x</sub>, and halides). The  
81 total evolved CO<sub>2</sub> is measured using a capacitance manometer (MKS Type 622A, 0-100  
82 torr, ±0.25% full-range precision), diluted with <sup>14</sup>C-dead CO<sub>2</sub> to facilitate graphitization  
83 for AMS analysis (typical samples are only 20-50 μg of C, blanks 5-10 μg C), and split  
84 into two breakseals for AMS and δ<sup>13</sup>C measurement. The AMS split is then converted to  
85 graphite using catalytic reduction following Slota (1987). For data presented here, the  
86 <sup>14</sup>C/<sup>13</sup>C ratio is measured by both AMS facilities.

## 87 Blank Measurements

88 All measurements (atoms and atoms g<sup>-1</sup>) reported below were converted from  
89 fraction modern values following the procedure outlined in Hippe et al. (in press). The  
90 δ<sup>13</sup>C correction included in the AMS laboratory reported fraction modern values is  
91 removed, as is reporting of the fraction modern value relative to 1950 AD. This yields  
92 carbon isotopic ratios relative to the isotopic ratio of the standard used in the AMS  
93 measurement (Ox-II here). Reported averages and uncertainties are arithmetic means and  
94 standard deviations. Sample concentrations are corrected for the long-term average blank.

95 Contamination from atmospheric, organic, and inorganic <sup>14</sup>C sources is  
96 potentially a large source of the measured <sup>14</sup>C in a sample. The measurement of

97 numerous process blanks with stable and low background levels is therefore critical to  
98 maximizing precision, confidence in the blank correction, and lowering the detection  
99 limit. The practice of bracketing samples, approximately every five, with measurements  
100 of the process blank are needed, because process blank measurements cannot be done  
101 simultaneously with sample extraction. Figure 1 shows the evolution of blank  
102 measurements at LDEO through time. The observed trend displays an overall reduction  
103 in background  $^{14}\text{C}$  by ~60%. It is difficult to attribute the reduction in background to a  
104 given cause except for more thorough cleaning of the sacrificial quartz sleeve prior to  
105 insertion into the furnace, along with diligent cleaning and handling of other quartz  
106 implements entering the furnace. This conclusion is supported by the observation that  
107 blank levels show a positive correlation with the total mass of carbon evolved during the  
108 extraction procedure (Figure 2). It may however simply be due to progressive removal of  
109 contaminant carbon in the line itself through repeated use, as has been suggested for other  
110 similar *in situ*  $^{14}\text{C}$  systems (Fülöp et al., 2010; Hippe et al., 2009). Regardless of the exact  
111 cause of improvement in process blank levels, process blanks since January 2010 range  
112 between  $54 \pm 13 \times 10^3$  and  $179 \pm 51 \times 10^3$  atoms  $^{14}\text{C}$  with an average and standard deviation of  
113  $125 \pm 42 \times 10^3$  atoms  $^{14}\text{C}$  ( $n=9$ ) for these blanks. Blanks from January 2010 and later are  
114 used as this represents the beginning of consistent use of the line and therefore likely  
115 represent the true characteristic value for the process blank. Our process blank level is  
116 commensurate with blank levels reported for similar line designs (Fülöp et al., 2010;  
117 Lifton et al., 2001; Miller et al., 2006; Pigati, 2004).

118 Capabilities

119 Figure 3 shows the relationship between total uncertainty and  $^{14}\text{C}$  concentration  
120 measured at LDEO covering a range between  $10 \times 10^3$  and  $680 \times 10^3$  atoms  $\text{g}^{-1}$ . The overall  
121 relationship is roughly an inverse exponential. At concentrations greater than  
122 approximately  $100 \times 10^3$  atoms  $\text{g}^{-1}$  there is no strong correlation. The observed relationship  
123 is a result of both AMS measurement uncertainty and the large influence of the blank  
124 correction on low concentration samples. At concentrations  $>200 \times 10^3$  atoms  $\text{g}^{-1}$ , the  
125 resulting analytical uncertainty is dominated by AMS counting statistics; however, as  
126 concentrations fall below the “threshold” of  $\sim 100 \times 10^3$  atoms  $\text{g}^{-1}$ , analytical uncertainties  
127 increase exponentially as a result of a large blank correction, in addition to any larger  
128 AMS uncertainties. From this, the effective detection limits of *in situ*  $^{14}\text{C}$  measurements  
129 for our line can be established. Two samples in particular show that concentrations below  
130  $\sim 30 \times 10^3$  atoms  $\text{g}^{-1}$  yield very large uncertainties and in some cases are not statistically  
131 different from 0.

### 132 CRONUS-A Measurements

133 To assess intra-laboratory measurement variability, we measured one of the  
134 CRONUS-Earth intercomparison materials, CRONUS-A. Results of six measurements of  
135 CRONUS-A by two operators over an approximately two-year period are presented in  
136 Table 2 and Figure 4. All measurements are indistinguishable within 1-sigma  
137 uncertainties with the exception of one low measurement. The resulting mean  
138 concentration including all measurements is  $652 \pm 33 \times 10^3$  atoms  $\text{g}^{-1}$ . We interpret the  
139 standard deviation of  $\sim 5\%$  to represent the intra-laboratory reproducibility of *in situ*  $^{14}\text{C}$   
140 extractions from samples with a similar concentration to CRONUS-A. It is possible that a  
141 lower concentration will yield more scatter; however, a lower concentration

142 intercomparison material (CRONUS-N) yields effectively zero  $^{14}\text{C}$  atoms  $\text{g}^{-1}$  for the *in*  
143 *situ*  $^{14}\text{C}$  concentration and therefore the relationship between scatter and concentration is  
144 unable to be established. A more recently developed intercomparison material,  
145 CRONUS-R, should yield a lower measured concentration than CRONUS-A, and  
146 hopefully greater than CRONUS-N, and may provide insight into any correlation  
147 between concentration and scatter.

## 148 Conclusions

149 We have successfully constructed an *in situ*  $^{14}\text{C}$  extraction laboratory at Lamont-  
150 Doherty Earth Observatory based on the designs of Pigati (2004) and Lifton et al. (2001),  
151 significantly increasing the potential number of *in situ*  $^{14}\text{C}$  measurements made. During  
152 the last two years, blank levels have been low, commensurate with similar laboratories,  
153 and show good stability. Potential analytical uncertainty is very good and shows little  
154 dependence on concentration above a threshold value of about  $100 \times 10^3$  atoms  $\text{g}^{-1}$ . Intra-  
155 laboratory scatter, as determined from repeat measurements of an inter-laboratory  
156 comparison material is  $\sim 5\%$ . Development of the Lamont-Doherty Earth Observatory  
157 represents a significant advancement in the potential use of *in situ*  $^{14}\text{C}$  in studies of earth  
158 surface processes and landform dating, with many applications only presently being  
159 realized.

## 160 Acknowledgements

161 We graciously thank the support and assistance of Nat Lifton during laboratory  
162 development. Without his knowledge none of this would have been possible. We also  
163 thank Tim Jull and the rest of the staff at the University of Arizona AMS facility, as well

164 as Tom Guilderson and the staff of the Lawrence-Livermore Center for AMS. This is  
165 LDEO Publication xxxx.

## 166 References

- 167 Anderson, R.K., Miller, G.H., Briner, J.P., Lifton, N.A., DeVogel, S.B., 2008. A  
168 millennial perspective of Arctic warming from  $^{14}\text{C}$  in quartz and plants emerging from  
169 beneath ice caps. *Geophys. Res. Lett.* 35, doi: 10.1029/2007GL03057.
- 170 Brook, E.J., Brown, E.T., Kurz, M.D., Ackert, J., Robert P., Raisbeck, G., Yiou, F., 1995.  
171 Constraints on age, erosion, and uplift of Neogene glacial deposits in the Transantarctic  
172 Mountains determined from in situ cosmogenic  $^{10}\text{Be}$  and  $^{26}\text{Al}$ . *Geology* 23, 1063-1066.
- 173 Dugan, B., Lifton, N., Jull, A.J.T., 2008. New production rate estimates for in situ  
174 cosmogenic C-14. *Geochim. Cosmochim. Acta* 72, A231-A231.
- 175 Fülöp, R.-H., Bishop, P., Fabel, D., Cook, G.T., Schnabel, C., Naysmith, P., Xu, S., 2009.  
176 Determining amounts and timing of soil erosion using in situ cosmogenic  $^{14}\text{C}$  and  $^{10}\text{Be}$ .  
177 *Geochimica Et Cosmochimica Acta Supplement* 73, A403.
- 178 Fülöp, R.H., Naysmith, P., Cook, G.T., Fabel, D., Xu, S., Bishop, P., 2010. Update on the  
179 Performance of the Suerc in Situ Cosmogenic C-14 Extraction Line. *Radiocarbon* 52,  
180 1288-1294.
- 181 Goehring, B.M., Schaefer, J.M., Lifton, N., Jull, A.J.T., 2008. Progress and Initial Results  
182 from the Lamont-Doherty Earth Observatory in situ Carbon-14 Extraction Laboratory,  
183 Accelerator Mass Spectrometry 11 Meeting, Rome, Italy.
- 184 Goehring, B.M., Schaefer, J.M., Schluechter, C., Lifton, N.A., Finkel, R.C., Jull, A.J.T.,  
185 Akçar, N., Alley, R.B., 2011. The Rhone Glacier was smaller than today for most of the  
186 Holocene. *Geology* 39, 679-682.
- 187 Handwerger, D.A., Cerling, T.E., Bruhn, R.L., 1999. Cosmogenic  $^{14}\text{C}$  in carbonate rocks.  
188 *Geomorph.* 27, 13-24.
- 189 Hippe, K., Kober, F., Baur, H., Ruff, M., Wacker, L., Wieler, R., 2009. The current  
190 performance of the in situ  $^{14}\text{C}$  extraction line at ETH. *Quat. Geochron.* 4, 493-500.
- 191 Hippe, K., Kober, F., Wacker, L., Fahrni, S.M., Ivy-Ochs, S., Akcar, N., Schluchter, C.,  
192 Wieler, R., in press. An update on in situ cosmogenic  $^{14}\text{C}$  analysis at ETH Zürich. *Nucl.*  
193 *Instrum. Methods.*
- 194 Hippe, K., Kober, F., Zeilinger, G., Ivy-Ochs, S., Maden, C., Wacker, L., Kubik, P.W.,  
195 Wieler, R., 2012. Quantifying denudation rates and sediment storage on the eastern  
196 Altiplano, Bolivia, using cosmogenic  $^{10}\text{Be}$ ,  $^{26}\text{Al}$ , and in situ  $^{14}\text{C}$ . *Geomorph.*
- 197 Lal, D., Pavich, M., Gu, Z.Y., Jull, A., 1996. Recent Erosional History of a Soil Profile  
198 Based on Cosmogenic In-Situ Radionuclides  $^{14}\text{C}$  and  $^{10}\text{Be}$ . *Geophysical Monograph* 95,  
199 371-376.
- 200 Lifton, N., Smart, D., Shea, M., 2008. Scaling time-integrated in situ cosmogenic nuclide  
201 production rates using a continuous geomagnetic model. *Earth Planet. Sci. Lett.* 268, 190-  
202 201.
- 203 Lifton, N.A., Jull, A.J.T., Quade, J., 2001. A new extraction technique and production  
204 rate estimate for in situ cosmogenic  $^{14}\text{C}$  in quartz. *Geochim. Cosmochim. Acta* 65, 1953-  
205 1969.



206 Matmon, A., Shaked, Y., Porat, N., Enzel, Y., Finkel, R., Lifton, N., Boaretto, E., Agnon,  
207 A., 2005. Landscape development in an hyperarid sandstone environment along the  
208 margins of the Dead Sea fault: Implications from dated rock falls. *Earth Planet. Sci. Lett.*  
209 240, 803-817.

210 Miller, G.H., Briner, J.P., Lifton, N.A., Finkel, R.C., 2006. Limited ice-sheet erosion and  
211 complex exposure histories derived from in situ cosmogenic  $^{10}\text{Be}$ ,  $^{26}\text{Al}$ , and  $^{14}\text{C}$  on Baffin  
212 Island, Arctic Canada. *Quat. Geochron.* 1, 74-85.

213 Pigati, J.S., 2004. Experimental Developments and Application of Carbon-14 and in situ  
214 Cosmogenic Nuclide Dating Techniques, Department of Geosciences. University of  
215 Arizona, Tucson, AZ, p. 188.

216 Pigati, J.S., Lifton, N.A., Jull, A.J.T., Quade, J., 2010. A Simplified In Situ Cosmogenic  
217  $^{14}\text{C}$  Extraction System. *Radiocarbon* 52, 1236-1243.

218 Schimmelpfennig, I., Schaefer, J., Goehring, B.M., Lifton, N., Putnam, A., 2012.  
219 Calibration of the in-situ  $^{14}\text{C}$  production rate in the Southern Alps, New Zealand. *J. Quat.*  
220 *Sci.* 27, 671-674.

221 Slota, P.J., Jr., Jull, A.J.T., Linick, T.W., Toolin, L.J., 1987. Preparation of small samples  
222 for  $^{14}\text{C}$  accelerator targets by catalytic reduction of CO. *Radiocarbon* 29, 303-306.

223 White, D., Fülöp, R.-H., Bishop, P., Mackintosh, A., Cook, G., 2011. Can in-situ  
224 cosmogenic  $^{14}\text{C}$  be used to assess the influence of clast recycling on exposure dating of  
225 ice retreat in Antarctica? *Quat. Geochron.* 6, 289-294.

226  
227

## Tables

Table 1. Process blank measurement information. Columns are the volume of CO<sub>2</sub> extracted from the sample, mass of carbon extracted, volume of the diluted sample, measured fraction modern, and number of <sup>14</sup>C atoms. Fm values measured relative to Ox-II. All blank measurements assume a δ<sup>13</sup>C value of -17.6±0.17 ‰ unless otherwise noted, which is based on numerous measurements of our dilution CO<sub>2</sub> and effectively dominates the measured δ<sup>13</sup>C value due to the large dilution factor. <sup>14</sup>C measurements were either made at the University of Arizona (UA) or the Lawrence-Livermore Center for Accelerator Mass Spectrometry (CAMS).

Date	AMS Lab	V <sub>CO2</sub> (10 <sup>-2</sup> cc STP)	Mass C (μg)	V <sub>diluted</sub> (10 <sup>-2</sup> cc STP)	Fm <sub>Meas</sub>	δ <sup>13</sup> C (‰)	<sup>14</sup> C (10 <sup>3</sup> atoms)
7/7/08	UA	2.36±0.02	12.65±0.08	131.91±0.88	0.0236±0.0006	-	903.79±54.31
7/9/08	UA	2.67±0.02	14.28±0.10	131.26±0.88	0.0138±0.0005	-	494.67±52.40
					Average	-	699.23±289.29
1/26/09	UA	1.50±0.02	8.01±0.09	127.62±1.46	0.0075±0.0012	-	212.80±67.74
2/19/09	UA	1.91±0.02	10.21±0.12	158.87±1.82	0.0097±0.0012	-	391.38±83.90
					Average	-	302.09±126.27
1/30/10	UA	1.73±0.01	9.24±0.08	251.56±2.13	0.0035±0.0002	-17.474±0.004	169.05±93.36
2/11/10	UA	1.52±0.02	8.16±0.09	147.07±1.68	0.0051±0.0003	-17.569±0.007	144.48±56.28
3/5/10	UA	1.24±0.01	6.63±0.08	114.41±1.32	0.0057±0.0002	-	132.90±43.07
3/29/10	UA	1.78±0.02	9.54±0.11	137.18±1.57	0.0059±0.0002	-	178.68±51.29
7/28/10	CAMS	1.29±0.02	6.89±0.08	142.17±1.64	0.0045±0.0001	-	89.28±13.02
1/11/11	CAMS	1.27±0.01	6.80±0.08	140.45±1.61	0.0037±0.0001	-	53.65±12.76
1/13/11	CAMS	1.30±0.02	6.94±0.08	138.01±1.59	0.0043±0.0001	-	79.44±12.71
5/11/11	CAMS	1.57±0.02	8.41±0.10	134.64±1.54	0.0061±0.0001	-	152.88±12.88
6/1/11	CAMS	1.67±0.02	8.93±0.10	137.81±1.58	0.0053±0.0001	-	121.66±13.12
					Average	-	124.67±42.56

Table 2. Measurements of the CRONUS-A intercomparison material. Columns are as in Table 1, except showing concentrations (atoms g<sup>-1</sup>), rather than total atoms. δ<sup>13</sup>C values for each sample are indicated, otherwise they are assumed to be -17.74±0.17 ‰, which is derived from the average of δ<sup>13</sup>C values measured in quartz samples, but effectively is dominated by our dilution CO<sub>2</sub>.

Sample ID	AMS Lab	Qtz Mass (g)	V CO <sub>2</sub> (10 <sup>-2</sup> cc STP)	Mass C (μg)	V <sub>diluted</sub> (10 <sup>-2</sup> cc STP)	F <sub>m Meas</sub>	δ <sup>13</sup> C (‰)	<sup>14</sup> C (10 <sup>3</sup> at g <sup>-1</sup> )
CRONUS-A <sup>1</sup>	UA	5.0045	6.15±0.07	32.96±0.38	172.36±1.97	0.067±0.0013	-17.61±0.02	642.68±32.80
CRONUS-A-2 <sup>1</sup>	UA	4.6503	6.00±0.07	32.11±0.37	125.00±1.43	0.075±0.0010	-17.49±0.01	591.54±17.88
CRONUS-A-NM-1	CAMS	4.9739	6.14±0.07	32.89±0.38	138.11±1.58	0.081±0.0005	-	657.51±12.58
CRONUS-A-NM-2	CAMS	4.9912	6.71±0.08	35.94±0.41	143.73±1.66	0.080±0.0004	-	679.54±12.69
CRONUS-A-3-19-11	CAMS	5.0050	7.59±0.09	40.66±0.47	143.30±1.64	0.081±0.0004	-	677.98±12.44
CRONUS-A-3-28-11	CAMS	5.0211	7.52±0.09	40.27±0.46	142.73±1.63	0.080±0.0004	-	664.33±12.29
							Average	652.26±32.7

<sup>1</sup> Blank correction based on blanks completed in 2009. All other CRONUS-A measurements are corrected for the mean blank 2010 and later.

## Figure Captions

Figure 1. Plot of blank measurements versus time. Trend shows gradual improvement in blank levels and overall improvement in consistency. In all figures, errors are shown at one-sigma.

Figure 2. Blank levels versus total carbon evolved during a process blank. A correlation is observed between carbon mass and number of  $^{14}\text{C}$  atoms.

Figure 3. Analytical uncertainty versus sample concentration.

Figure 4. Plot of all measurements of the CRONUS-A intercomparison material. Solid line indicates arithmetic mean of all values, shading is one standard deviation, dashed line indicates two standard deviations.

Figure 1

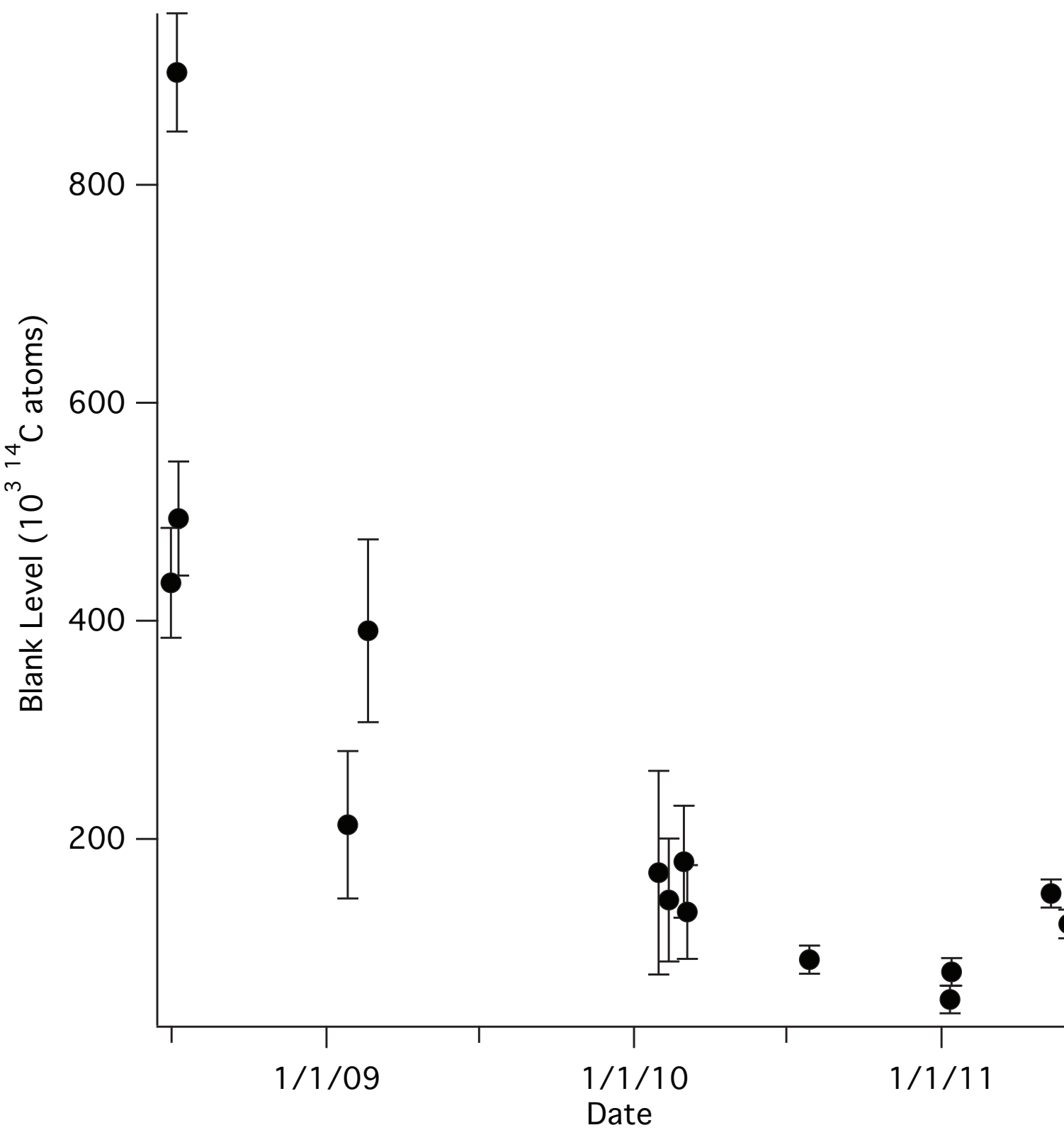


Figure 2

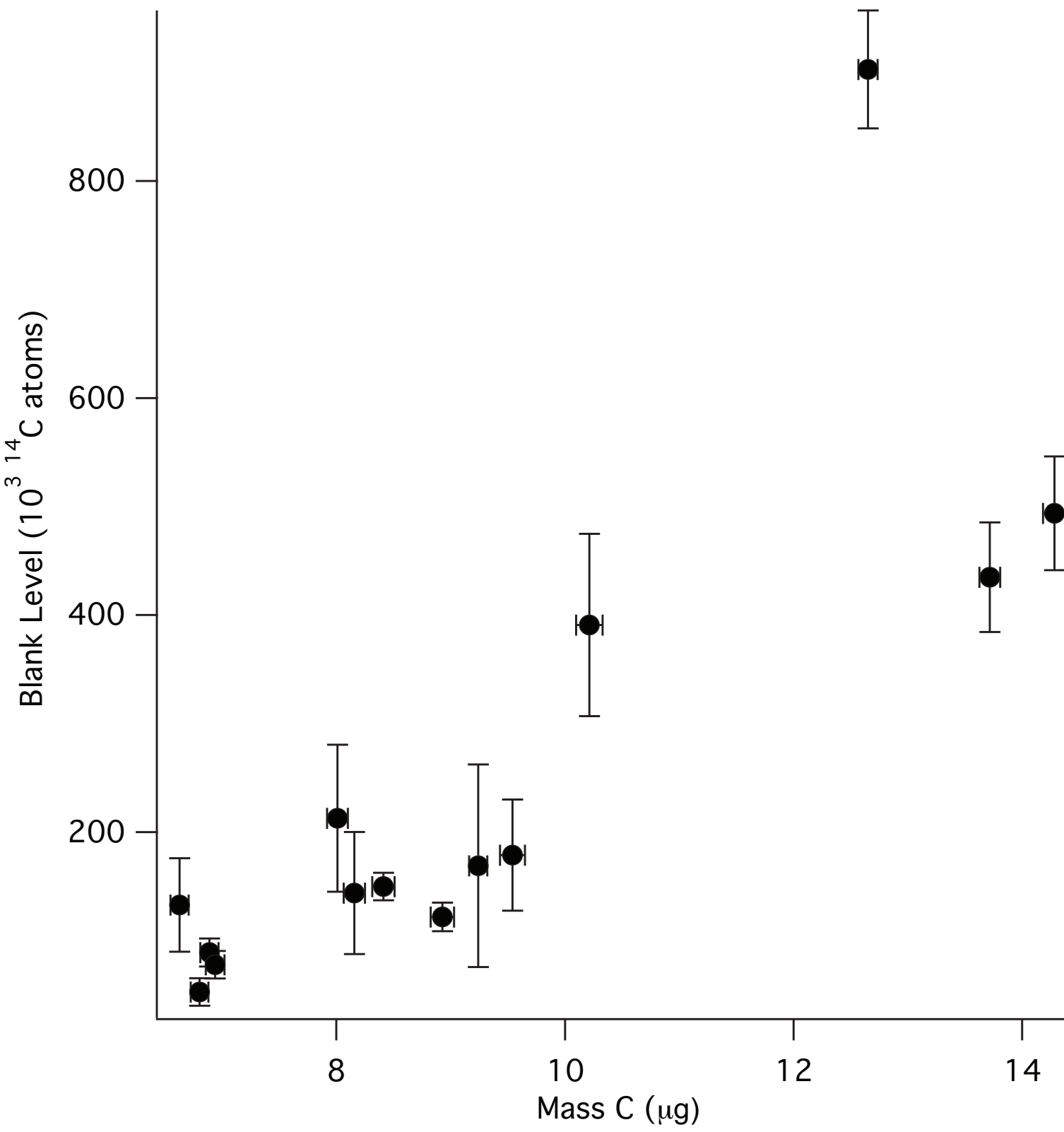


Figure 3

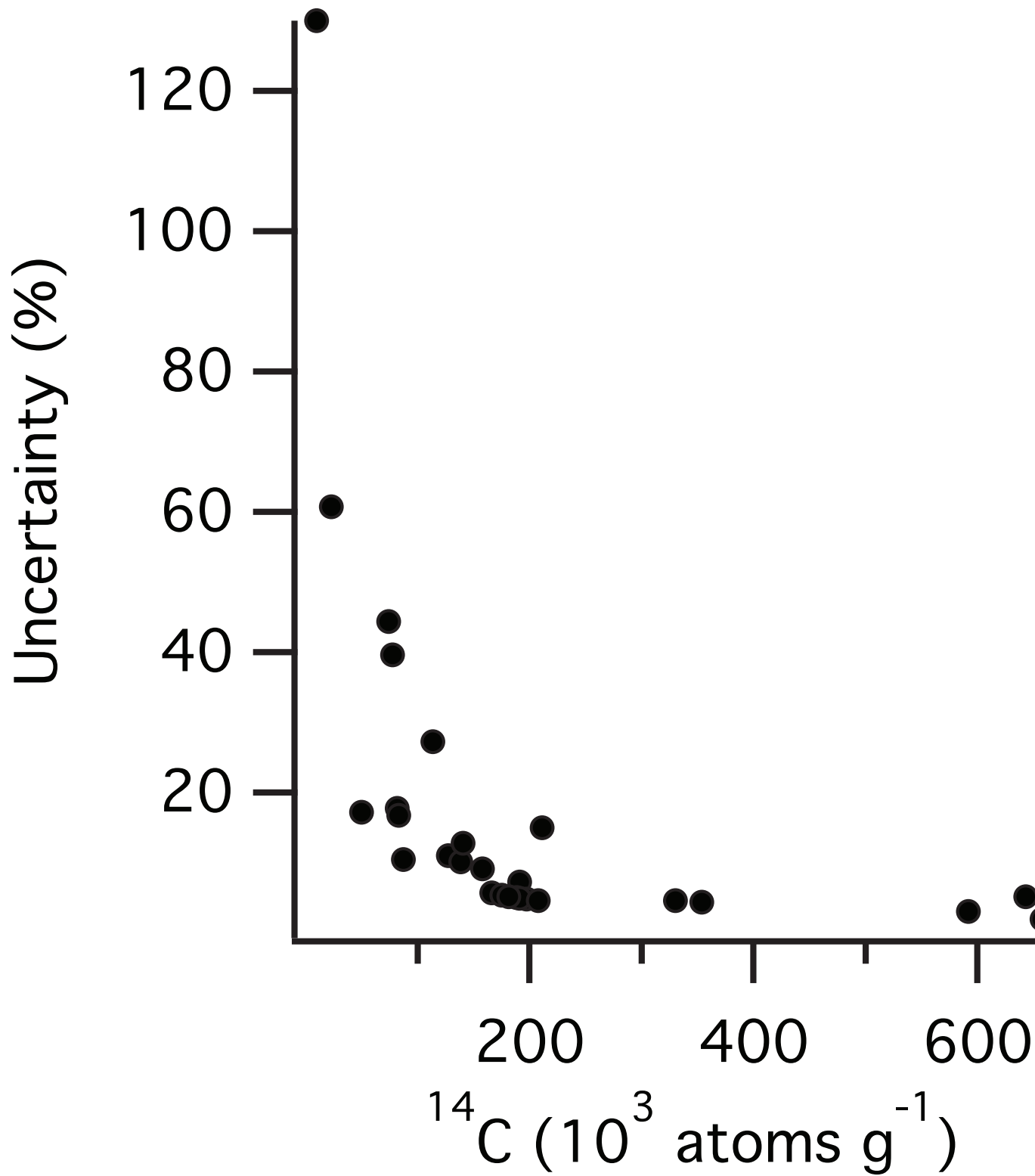


Figure 4

